



**HAL**  
open science

# Combined effects of particle-wall interactions and turbulent dispersion in gas-solid flows using accurate Lagrangian stochastic modelling

Mohammed Khalij, Anne Tanière, Benoit Oesterlé

► **To cite this version:**

Mohammed Khalij, Anne Tanière, Benoit Oesterlé. Combined effects of particle-wall interactions and turbulent dispersion in gas-solid flows using accurate Lagrangian stochastic modelling. 5th Word Congress on Computational Mechanics, 2002, Vienne, Austria. hal-03542596

**HAL Id: hal-03542596**

**<https://hal.univ-lorraine.fr/hal-03542596v1>**

Submitted on 25 Jan 2022

**HAL** is a multi-disciplinary open access archive for the deposit and dissemination of scientific research documents, whether they are published or not. The documents may come from teaching and research institutions in France or abroad, or from public or private research centers.

L'archive ouverte pluridisciplinaire **HAL**, est destinée au dépôt et à la diffusion de documents scientifiques de niveau recherche, publiés ou non, émanant des établissements d'enseignement et de recherche français ou étrangers, des laboratoires publics ou privés.

# **Combined effects of particle-wall interactions and turbulent dispersion in gas-solid flows using accurate Lagrangian stochastic modelling**

**M. Khalij, A. Tanière, and B. Oesterlé\***

LEMTA (LUMEN Group) – UMR 7563 CNRS, Université Henri Poincaré - Nancy 1  
ESSTIN, 2 rue Jean Lamour, 54519 Vandoeuvre-lès-Nancy, France  
e-mail: [oeesterbe@esstin.uhp-nancy.fr](mailto:oeesterbe@esstin.uhp-nancy.fr)

**Key words:** turbulence, particle dispersion, stochastic Lagrangian model, wall collisions

## **Abstract**

The behaviour of the particulate phase in a turbulent gas-solid channel flow is investigated by means of an improved Lagrangian stochastic model combined with realistic treatment of saltation phenomena using an irregular bouncing model for particle-wall collisions. Such particle-wall interaction mechanisms, which are difficult to include in two-fluid (Eulerian-Eulerian) models, may be accurately described by means of the Eulerian-Lagrangian approach. In that sense the present study is a preliminary step towards improvement of the formulation of wall boundary conditions needed in two-fluid models.

Particles are numerically tracked by predicting the instantaneous fluid velocity at the discrete particle location using a modified Langevin model, which takes the anisotropy and the non homogeneous character of the turbulence into account. Comparisons with available experimental data are provided, and examples illustrating the effects of the collision parameters upon the particle mean and r.m.s. velocities, kinetic stresses and concentration distribution in channel flows are given. The effect of irregular bouncing upon the relationships between various particle velocity correlations at the wall is examined and discussed with relevance to boundary conditions used in Eulerian two-fluid models.

## 1 Introduction

A great number of experimental and numerical investigations have been devoted to the study of the motion and distribution of solid particles conveyed in wall-bounded turbulent flows. Most of them deal with gas-solid channel flows [1-4]. Computational models aimed at numerically predicting such dispersed two-phase flows include the so-called Eulerian-Lagrangian approaches and the two-fluid models or Eulerian-Eulerian methods, the latter being more effective and less time consuming. However, some details of the dispersed phase flow are much more accurately described by the Lagrangian technique, which can therefore be used as a tool for improving some modelling aspects needed in two-fluid models, like the particulate phase wall conditions [5-7], which may have significant consequences on pressure drop predictions for instance.

This is one of the purposes of this work, where an Eulerian-Lagrangian approach is used to simulate a gas-solid channel flow in order to examine the properties of the particulate phase motion as competing effects of wall collisions and turbulence are expected. Additionally, the need of accurate modelling of near-wall turbulence effects is put forward, and an original model is used to predict the anisotropic turbulent dispersion of solid particles, including improvements in the assessment of the required time scales of the fluid flow.

In such wall bounded flows, the prevailing effect of inter-particle collisions compared with turbulence modulation has been pointed out by many investigators (see [2,3,8,9]). This is the reason why such particle-to-particle interactions are taken into account in the present simulations, whereas turbulence modulation is neglected since our main goal is to characterize the near-wall behaviour of the dispersed phase at moderate loading. Furthermore, the boundary conditions that we are investigating, which consist in relationships between various 2<sup>nd</sup> and 3<sup>rd</sup> order particle velocity correlations, do not depend on the flow properties but only on the particle-wall collision parameters.

After checking the capability of the numerical code in two opposite cases, namely a saltation dominated horizontal flow and a vertical channel flow where the particle motion is mainly controlled by turbulence and inter-particle collisions, we focus on the effect of irregular bouncing upon the properties of the particulate flow. In the following sections, the Eulerian-Lagrangian simulation is first presented, including some details about the associated dispersion and collision models. Some numerical results are then presented and discussed concerning the combined effect of turbulence and particle-wall interactions, and the effect of the collision parameters upon the relationships between various particle velocity correlations at the wall is examined.

## 2 Simulation overview

### 2.1 Use of an anisotropic Low-Reynolds model for the fluid phase

The fully developed channel flow is described by the usual Reynolds-averaged Navier-Stokes equations. It is assumed that the suspension flow is dilute enough for the effect of the particulate phase on the fluid flow properties to be negligible. Closure is achieved through an anisotropic Low-Reynolds  $k$ - $\varepsilon$  model, where the fluid Reynolds stresses are modelled by means of a non linear eddy viscosity model as proposed by Rokni & Sunden [10]. In order to account for the near-wall effects, the turbulence model has been modified as recommended by Myong & Kasagi [11]. The corresponding Low-Reynolds model requires that the first node be located very close to the wall, namely  $y^+ < 0.6$ . Therefore, numerical calculations have been carried out using a stretched grid in the wall-normal direction, with 50 nodes along the half channel width, and the first grid node located at  $y^+ \cong 0.4$ .

## 2.2 Lagrangian modelling of the dispersed phase flow

### 2.2.1 Outlines of particle trajectory calculation

The solid phase motion is simulated by tracking a large number of particles injected in the gas flow field. Particles are assumed to be rigid and spherical. Due to particle-wall and particle-particle interactions, which are not supposed to be frictionless, particles may be subjected to significant rotational motion, which is to be taken into account in expressing the particle-fluid interactions. The particle motion is therefore described by a set of six equations (linear and angular momentum conservation). Besides the quasi-stationary drag force, which is expressed according to usual standard correlations for the drag coefficient in terms of the sphere Reynolds number, particles are experiencing a torque and a lift force which may be of significant importance, particularly for large particles (see [12]). All these fluid-particle interaction forces (and torque) involve the instantaneous velocity of the fluid at the particle location. Non-stationary contributions to the drag force, such as history force, added mass force and displaced force, were neglected, owing to the high particle-to-fluid density ratio. Mainly due to the lack of available data for particle Reynolds number exceeding unity, the shear and wall induced lift forces are also ignored, although this point might require further investigation.

Periodic boundary conditions are used between the inlet and outlet sections of the channel since the two-phase flow is assumed to be fully developed. The trajectory computation is reinitialized after each collision with the wall or with another particle. Simulation of such collisions requires some empirical parameters such as the static and kinetic friction factors  $f_s$  and  $f$ , and the coefficient of restitution  $e$ , which are needed to express the particle translational and rotational velocities after the collision using the impulsive equations and Coulomb's law.

For particle-wall collisions, the so-called "virtual wall" model of Sommerfeld [13,14] is used in order to account for the effect of wall roughness and particle shape (departure from sphericity). In this model, the actual wall is replaced by a virtual wall, whose inclination angle obeys a Gaussian distribution with given standard deviation  $\gamma$  and zero mean value. The so-called shadow effect is included in the model. The restitution and friction coefficients are fixed for each case, and the examples given in Section 3 focus on the effect of the virtual wall parameter  $\gamma$  and its consequences upon the particle mean velocities, kinetic stresses and concentration distribution. Particular attention is paid to the relationships between the components of the particle velocity covariance matrix at the wall, which are required in order to fix the boundary conditions in two-fluid models.

In order to avoid handling the particle-particle interactions in a deterministic way, which requires to simultaneously compute the trajectories of all the particles present in the flow domain (a method limited by present computer capacities due to the huge number of particles in actual flows), interparticle collisions are taken into account according to the probabilistic method suggested by Oesterlé & Petitjean [15]. In this method, the occurrence of a collision is decided, at each time step, according to a collision probability depending on the local concentration and properties of the two-phase flow. The collision probability is obtained from the expression of the inter-particle collision frequency corrected to account for the correlated motion of neighbouring particles [16]. In case of collision, the tracked particle hits a standard particle whose translational and rotational velocities are determined using the average and r.m.s. values of the velocities of the solid phase. The precise position of the point of impact is chosen according to a uniform probability on the disc corresponding to the effective collision cross-section. This allows to compute the velocity components after collision, and therefore to restart the trajectory calculation process.

Once the Eulerian calculation of the fluid flow unknowns has been achieved, series of Lagrangian steps (with  $10^6$  particle trajectories for each step) are carried out with the fluctuating quantities of the fluid being calculated according to the dispersion model described below, using the data provided by the Eulerian calculation. In the first Lagrangian step, inter-particle collisions are not considered. From

the second Lagrangian step, such collisions are included by means of the probabilistic method, using the concentration and velocities obtained in the previous Lagrangian step.

### 2.2.2 Dispersion model

In order to reproduce the effect of the fluid turbulence upon the particle motion, the instantaneous fluid velocity along the particle path (the velocity of the fluid "seen") has to be properly assessed to express the instantaneous forces acting on the particle. Here, a direct method is used to predict the time rate of change of the velocity of the fluid seen : basically, a first-order autoregressive process is used to predict the instantaneous fluid velocity seen by a particle at time level  $t = n\Delta t$  from the fluid velocity seen by the same particle at time level  $t - \Delta t = (n-1)\Delta t$  :

$$u_{f_i n} = u_{f_i n-1} e^{-\Delta t/T_i^*} + \psi_{i_n} \quad (1)$$

where  $u_{f_i n}$  is the  $i$ -component of the velocity fluctuation of the fluid at the discrete particle location at time  $n\Delta t$ ,  $T_i^*$  is the integral time scale of the fluid seen in the  $i$ -direction, and the  $\psi_{i_n}$  are centered Gaussian variables satisfying  $\langle \psi_{i_n} \psi_{i_n-p} \rangle = 0$  for any integer  $p \neq 0$ .

Anisotropy can be introduced into the stochastic process by linking the white noise disturbances  $\psi_{i_n}$  ( $i=1,3$ ) in order to satisfy the prescribed values of the Reynolds stresses (which are known from the Eulerian calculation). From Equ.(1), we get the conditions to be fulfilled by the covariances (under local homogeneity assumption in order that the process be stationary) :

$$\langle \psi_{i_n} \psi_{j_n} \rangle = \left( 1 - \exp\left(-\Delta t \left(\frac{1}{T_i^*} + \frac{1}{T_j^*}\right)\right) \right) \langle u_{f_i} u_{f_j} \rangle \quad (2)$$

A simple procedure to generate such random numbers  $\psi_{i_n}$  is to select  $\psi_{1_n}$  from a normal p.d.f. with zero mean and variance  $\langle \psi_{1_n}^2 \rangle = (1 - \exp(-2\Delta t/T_1^*)) \langle u_{f_1}^2 \rangle$ , and to build  $\psi_{2_n}$  and  $\psi_{3_n}$  by  $\psi_{2_n} = a_0 \varphi + a_1 \psi_{1_n}$  and  $\psi_{3_n} = b_0 \chi + b_1 \psi_{1_n} + b_2 \psi_{2_n}$ , where  $\varphi, \chi$  are independent Gaussian variables with zero mean and variance unity, and the coefficients  $a_k, b_k$  are deduced from Equ.(2).

Under conditions of non homogeneous turbulence, it is necessary to take the variation of the fluid Reynolds stresses into account to avoid the spurious drift of fluid particles towards the low turbulence intensity regions [17,18]. In our channel flow configuration, the corresponding correction involves the  $y$ -derivatives of the fluid Reynolds stress and wall-normal velocity variance, according to :

$$u_{f_x n} = u_{f_x n-1} \exp\left(-\frac{\Delta t}{T_x^*}\right) + \psi_{x_n} + \frac{\partial \langle u_{f_x} u_{f_y} \rangle}{\partial y} T_x^* \left(1 - \exp\left(-\frac{\Delta t}{T_x^*}\right)\right) \quad (3)$$

$$u_{f_y n} = u_{f_y n-1} \exp\left(-\frac{\Delta t}{T_y^*}\right) + \psi_{y_n} + \frac{\partial \langle u_{f_y}^2 \rangle}{\partial y} T_y^* \left(1 - \exp\left(-\frac{\Delta t}{T_y^*}\right)\right) \quad (4)$$

$$u_{f_z n} = u_{f_z n-1} \exp\left(-\frac{\Delta t}{T_z^*}\right) + \psi_{z_n}, \quad (5)$$

where  $x, y, z$  denote the streamwise, wall-normal and spanwise directions, respectively.

The integral Lagrangian time scales  $T_i^*$  of the fluid seen by the discrete particles are evaluated following the proposals of Wang & Stock [19], which may yield acceptable estimates even in case of our non-homogeneous anisotropic channel flow, provided that the fluid Lagrangian time scales  $T_{Li}$  and moving Eulerian time scales  $T_{mEi}$  are properly assessed in terms of the  $y$ -location along the

channel height, as described later.

First, the integral time scales of the fluid seen when no external force is acting are computed by :

$$T_{0i}^* = T_{mEi} \left( 1 - \left( 1 - \frac{T_{Li}}{T_{mEi}} \right) (1 + St_i)^{-0.4(1+0.01St_i)} \right) \quad (6)$$

where the inertia effect is introduced through the particle Stokes numbers  $St_i = \tau_p / T_{mEi}$ ,  $\tau_p$  being the particle relaxation time. Crossing trajectories effects are then introduced by expressing the time scales  $T_x^*, T_y^*, T_z^*$  in terms of  $T_{0i}^*$  and the mean drift velocity  $v_d$  (which is directed in the streamwise direction  $x$ ) :

$$T_x^* = T_{0x}^* \left( 1 + \left( \frac{T_{0x}^* v_d}{L_f} \right)^2 \right)^{-1/2}, \quad T_{y,z}^* = T_{0y,z}^* \left[ \left( 1 + \left( \frac{T_{0y,z}^* v_d}{L_f} \right)^2 \right)^{1/2} - \frac{T_{0y,z}^* v_d}{2L_f} \right] \left( 1 + \left( \frac{T_{0y,z}^* v_d}{L_f} \right)^2 \right)^{-1/2} \quad (7)$$

where  $L_f$  is the longitudinal integral length scale defined here by  $L_f = \sqrt{\langle u_{fz}^2 \rangle} T_{mEz}$ .

Now, the remaining unknowns are the fluid timescales  $T_{Li}$  and  $T_{mEi}$  in each direction. We will make use of a recent model [20] supported by DNS and LES investigations of channel flows to estimate the directional dependence as well as the wall distance dependence of the Lagrangian time scales. According to [20], the generally used empirical laws, which assume  $T_{Li} \propto \langle u_{fi}^2 \rangle / \varepsilon$ , are far from being satisfactory. The best way to evaluate the wall-normal Lagrangian time scale  $T_{Ly}$  is to express it using the proposal by Ushijima & Perkins [22], or alternatively by means of the eddy viscosity model which leads to  $T_{Ly} = -\langle u_{fx} u_{fy} \rangle / (\langle u_{fy}^2 \rangle dU/dy)$ . The streamwise and spanwise Lagrangian integral scales are then calculated from the model proposed in [20] :

$$T_{Lx} = T_{Ly} \frac{\langle u_{fx}^2 \rangle}{\langle u_{fy}^2 \rangle} \Psi, \quad T_{Lz} = T_{Ly} \frac{\langle u_{fz}^2 \rangle}{\langle u_{fy}^2 \rangle} \Psi, \quad \text{with } \Psi = \frac{1 + (\langle u_{fx} u_{fy} \rangle / \langle u_{fx}^2 \rangle)^2}{1 + (\langle u_{fx} u_{fy} \rangle / \langle u_{fy}^2 \rangle)^2} \quad (8)$$

The moving Eulerian time scales are deduced by prescribing a fixed value of the ratios  $\beta_i = T_{Li} / T_{mEi}$ , namely  $\beta_i \cong 0.6$ , which seems to be an acceptable estimate according to available LES and DNS results in channel flows [20,21].

## 3 Results and discussion

### 3.1 Comparison with available channel flow measurements

The predictions of the simulation are first compared with the experimental data of Kulick *et al* [1]. As mentioned above, trajectories have been computed assuming fully developed flow for fluid and particles ; the time step for the trajectory computation has been set to  $\Delta t = \min(\tau_p / 20, T_{L0} / 5, \tau_c / 10)$ , where  $T_{L0}$  is the transverse Lagrangian time scale at the channel center, and  $\tau_c$  is an estimate of the mean inter-particle collision time. The influence of the number of particles has been tested, showing that the computation of  $10^6$  particle trajectories in each Lagrangian loop is reasonable in order to get enough particles in each computational cell, at least for the statistics about the mean velocity and 2<sup>nd</sup> order correlations, even though better accuracy could have been obtained in the very near-wall cells by computing more trajectories.

In the experiments of Kulick *et al.* [1], mean and r.m.s. velocities profiles were measured in a downward vertical air-solid channel flow at moderate loading ratios  $\Phi$ , namely  $\Phi = 0.02, 0.1, 0.2$  and  $0.4$ . Particles were  $50 \mu\text{m}$  and  $90 \mu\text{m}$  glass beads and  $70 \mu\text{m}$  copper beads (nominal diameters). In fact the particles were polydispersed, however the present simulations have been performed assuming monodispersed particles. The width of the channel was  $0.04 \text{ m}$ , the fluid centerline velocity  $10.5 \text{ m/s}$  and the friction velocity was  $0.49 \text{ m/s}$ . The particle-wall collision parameters have been set to : kinetic and static friction factor  $f=f_s=0.3$ , coefficient of restitution  $e=0.95$ . Several values of the parameter  $\gamma$  (standard deviation of the virtual wall inclination) have been tested, showing that the main effect of irregular bouncing is upon the wall-normal r.m.s. velocity and the concentration profile : this will be discussed in the next section.

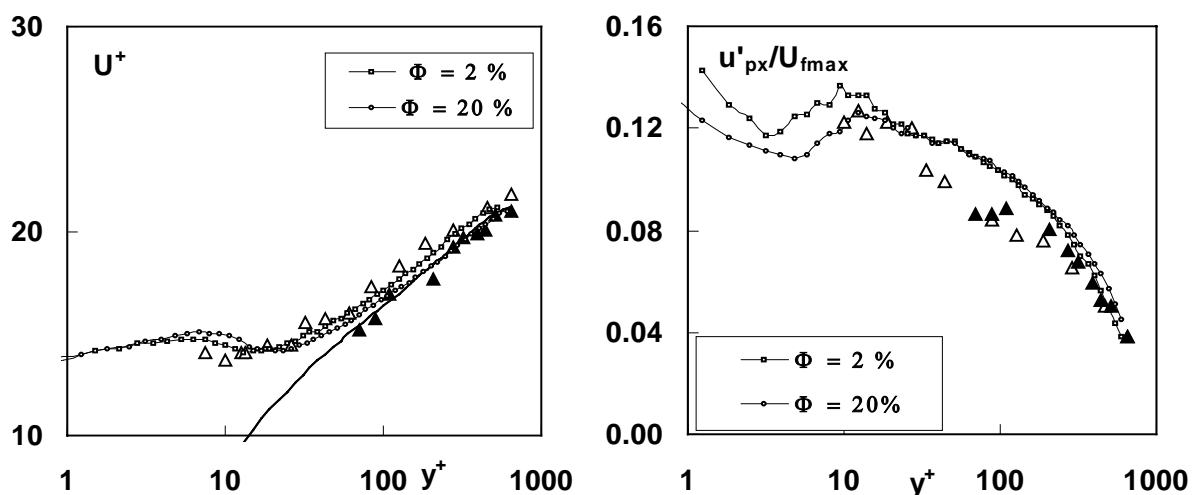


Figure 1: Particle mean and streamwise r.m.s. velocity profiles in a vertical channel. Comparison between the simulations (lines and small symbols, thin solid line : fluid) and the experimental results of Kulick *et al.* [1]( $\Delta$  :  $\Phi=2\%$ ,  $\blacktriangle$ :  $\Phi=20\%$ ).

Figure 1 displays a comparison between our simulations (for  $\gamma = 0.06$ ) and the experimental data for the  $50 \mu\text{m}$  glass particles used by Kulick *et al.* [1], showing that the effect of increasing loading upon the mean velocity profile is well reproduced by the computations, as well as the value of the mean particle velocity at the wall. In agreement with the measurements, the streamwise r.m.s. velocity is not found to be significantly altered by the solid concentration. It should be recalled that in the computations the effect of solid loading is introduced by inter-particle collisions, and that the effect of particles upon the fluid flow is not taken into account, thus confirming the prevailing role of inter-particle collisions in wall-bounded flows at low loading ratio.

### 3.2 The effect of the irregular bouncing parameter $\gamma$

In order to illustrate the effect of the irregular bouncing parameter, computations have been performed using the data of the above mentioned Kulick's experiments, as well as the horizontal channel measurements by Tsuji *et al.* [4].

The influence of  $\gamma$  in the experimental conditions of Kulick *et al.* [1] is shown in Fig.2, for the particle wall-normal r.m.s. velocity and concentration distribution ( $c_0$  is the concentration at channel center), which can be seen to be significantly affected. Due to increasing irregularity in particle-wall collisions, the wall-normal velocity fluctuations are intensified, resulting in a more uniform concentration profile. Compared to the results presented above, we can observe that the wall-normal

r.m.s. velocity is more difficult to accurately simulate, however the predictions obtained for  $\gamma = 0.06$  or  $\gamma = 0.08$  are nevertheless satisfactory, except very close to the wall where the fluctuating velocities are overestimated.

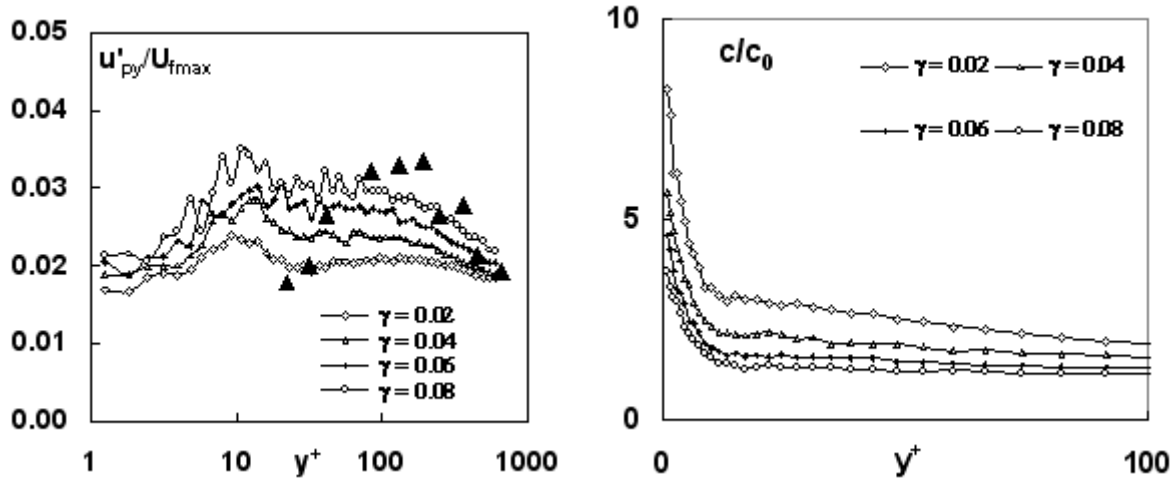


Figure 2: The influence of  $\gamma$  on the wall-normal r.m.s. velocity and the near-wall concentration distributions in the conditions of Kulick's experiments ( $\blacktriangle$ , loading 2%).

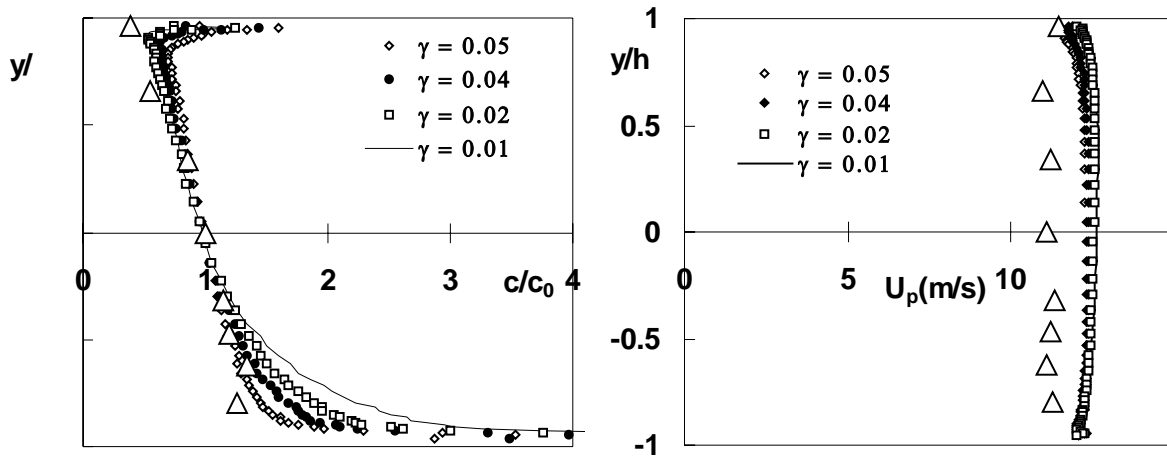


Figure 3: Concentration and particle mean velocity profiles in a horizontal channel. Comparison between the simulations (lines and small symbols) and the experimental results ( $\Delta$ ) of Tsuji *et al.* [4] at loading ratio  $\Phi = 1$  and mean air velocity 15 m/s.

The concentration profiles in the vertical channel were not measured in [1], however such profiles were investigated in the experiments of Tsuji *et al.* [4], together with the mean velocity profiles, in a horizontal air-solid channel flow. The height of the channel was 25 mm, the particles were polystyrene beads with diameter  $d=1$  mm and density  $\rho_p=1000$  kg·m<sup>-3</sup>. The mean air velocity was set at 7 or 15 m/s, and measurements were done at three loading ratios, namely  $\Phi = 1, 3$  and 5. According to the authors, the collision parameters were : kinetic friction factor  $f=0.4$ , coefficient of restitution  $e=0.8$ . A static friction factor  $f_s=0.5$  was assumed in our simulation, and several values of the parameter  $\gamma$  have been tested too. Since two-way coupling is not considered in the present simulations, comparison has



been carried out only for the lowest loading studied by Tsuji *et al.*, namely  $\Phi = 1$ . From Fig.3, it can be observed that acceptable agreement is obtained by the present simulation with  $\gamma \cong 0.05$ , even though the mean particle velocity is somewhat overestimated.

Again, the important effect of the nature of particle-wall interactions upon the concentration distribution is demonstrated in this example, and it is therefore questionable how such effects can be obtained by means of two-fluid computational models. Obviously, the answer lies in the formulation of proper boundary conditions at the wall for the particulate phase, however this problem has not yet been solved in case of irregular bouncing. This is the reason why it may be interesting to compare the present results from our Lagrangian simulation with the available theoretical relationships valid for spherical particles and smooth wall ( $\gamma = 0$ ). Such relationships, which were analytically derived by He & Simonin [5] and Sakiz & Simonin [6], involve the 2<sup>nd</sup> and 3<sup>rd</sup> order particle velocity correlations at a distance of one particle radius from the wall. Here, we restrict ourselves to the double correlations, which should satisfy the following relationships :

$$\langle u_{px}u_{py} \rangle_w = -f \langle u_{py}^2 \rangle_w \quad (9)$$

$$\langle u_{py}u_{pz} \rangle_w = 0 \quad (10)$$

It is worth mentioning that in the analytical derivation of such relationships, it is assumed that the sliding velocity is in the  $x$ -direction (negligible spanwise component of the impaction velocity for all particles), and that all collisions are sliding collisions. In order to make the simulation consistent with the latter assumption, the investigation of the particle boundary conditions has been carried out in enforcing sliding for all particle-wall collisions, therefore we may expect to obtain, at least approximately, quantitative agreement with equ. (9) on setting  $\gamma = 0$ . This is shown in Fig. 4, together with the effects of varying  $\gamma$  from 0 to 0.12, for two values of the friction coefficient,  $f = 0.2$  and  $f = 0.4$ . In each case, the ratio  $-\langle u_{px}u_{py} \rangle_w / \langle u_{py}^2 \rangle_w$  has been obtained through statistics over more than  $10^4$  particle-wall collisions, with the same particles as in Tsuji's experiments [4]. It can be seen from Fig. 4 that the predictions at  $\gamma = 0$  slightly exceed the theoretical value (which is  $f$ ), and that the ratio first increases with increasing  $\gamma$ , and then it decreases and finally seems to reach an asymptotic value which is of the order of  $0.7f$  to  $0.8f$ . Of course, such interesting but preliminary results need to be supplemented by further investigations in order to provide some means of taking the bouncing irregularities into account in two-fluid models.

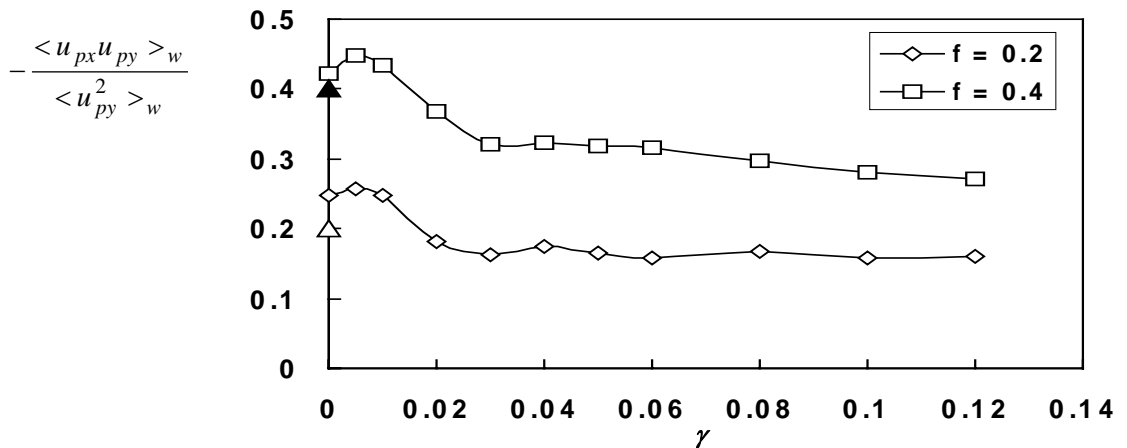


Figure 4: Illustration of the effect of irregular bouncing on the particulate phase wall condition. Plot of the ratio  $-\langle u_{px}u_{py} \rangle_w / \langle u_{py}^2 \rangle_w$  as a function of the irregular bouncing parameter  $\gamma$  (triangles are for the theoretical values at  $\gamma = 0$ ).

## 4 Conclusion

An improved Eulerian-Lagrangian technique has been presented for the computation of wall-bounded gas-solid flows. The method lies on accurate modelling of the near-wall behaviour of both the fluid phase (Low Reynolds anisotropic model) and the dispersed phase (particle turbulent dispersion, inter-particle collisions and particle-wall interactions). Satisfactory agreement has been obtained by comparison with available experimental data in vertical and horizontal channel flows.

Emphasis has been put on the effect of irregular bouncing due to wall roughness upon the properties of the particulate flow. It has been shown that the concentration and wall-normal r.m.s. velocity distributions are significantly altered by irregular bouncing, as are the wall boundary conditions which should be used in two-fluid models for the dispersed phase. Further computations are planned in order to get reliable statistics for such wall conditions, including the triple correlations and the correlations involving the angular velocity components.

### Acknowledgements

This work has been supported by INTAS (grant No 00-0309), which is gratefully acknowledged.

### References

- [1] J.D. Kulick, J.R. Fessler, J.K. Eaton, *Particle response and turbulence modification in fully developed channel flow*, J. Fluid Mech., 177 (1994), 109-134.
- [2] O. Simonin, Q. Wang, K. Squires, *Comparison between two-fluid model predictions and large eddy simulation results in a vertical gas-solid turbulent channel flow*, in Proc. 7<sup>th</sup> Int. Symp. Gas-Particle Flows, ASME Fluids Engng. Division Summer Meeting, Vancouver, 1997, ASME paper FEDSM97-3625.
- [3] T. Tanaka, Y. Yamamoto, M. Potthoff, Y. Tsuji, *LES of gas-particle turbulent channel flow*, in Proc. 7<sup>th</sup> Int. Symp. Gas-Particle Flows, ASME Fluids Engng. Division Summer Meeting, Vancouver, 1997, ASME paper FEDSM97-3630.
- [4] Y. Tsuji, Y. Morikawa, T. Tanaka, N. Nakatsukasa, M. Nakatani, *Numerical simulation of gas-solid two-phase flow in a two-dimensional horizontal channel*, Int J Multiphase Flow, 13 (1987), 671-684.
- [5] J. He, O. Simonin, *Modélisation numérique des écoulements turbulents gaz-solide en conduite verticale (Numerical modelling of dilute gas-solid turbulent flows in vertical channel)*. EDF Report n°HE-44/94/021A, Laboratoire National d'Hydraulique, Chatou, France (1994).
- [6] M. Sakiz, O. Simonin, *Development and validation of continuum particle wall boundary conditions using Lagrangian simulation of a vertical gas-solid channel flow*, in Proc. ASME FED Summer Meeting, 3<sup>rd</sup> ASME/JSME Joint Fluids Engng. Conf., San Francisco, 1999, ASME paper FEDSM99-7898.
- [7] X. Zhang, L.X. Zhou, *A two-fluid particle-wall collision model accounting for the wall roughness*, in M. Sommerfeld, ed., Proc. 10<sup>th</sup> Workshop on Two-Phase Flow Predictions, Merseburg, Germany, 2002, pp. 44-51.
- [8] K.D. Squires, O. Simonin, *Application of DNS and LES to dispersed two-phase turbulent flows*, in M. Sommerfeld, ed., Proc. 10<sup>th</sup> Workshop on Two-Phase Flow Predictions, Merseburg, Germany, 2002, pp. 152-163.

- [9] A.N. Volkov, Y.M. Tsirkunov, *CFD/Monte-Carlo simulation of collision-dominated gas-particle flows over bodies*, in *Proc. Joint US ASME-European Fluids Engng. Division Summer Meeting, Montreal, 2002*, ASME paper FEDSM2002-31222.
- [10] M. Rokni, B. Sunden, *Improved modelling of turbulent forced convective heat transfer in straight ducts*, *Trans. ASME, J. Heat Transfer*, 121 (1999), 712-719.
- [11] H.K. Myong, N. Kasagi, *A new approach to the improvement of k-e turbulence model for wall-bounded shear flows*, *JSME Int. Journal*, II-33 (1990), 63-72.
- [12] B. Oesterlé, T. Bui Dinh, *Experiments on the lift of a spinning sphere in a range of intermediate Reynolds numbers*, *Exp. Fluids*, 25 (1998), 16-22.
- [13] M. Sommerfeld, *Modelling of particle-wall collisions in confined gas-particle flows*, *Int. J. Multiphase Flow*, 18 (1992), 905-926.
- [14] M. Sommerfeld, N. Huber, *Experimental analysis and modelling of particle-wall collisions*, *Int. J. Multiphase Flow*, 25 (1999), 1457-1489.
- [15] B. Oesterlé, A. Petitjean, *Simulation of particle-to-particle interactions in gas-solid flows*, *Int. J. Multiphase Flow*, 19 (1993), 199-211.
- [16] J. Laviéville, O. Simonin, A. Berlemont, Z. Chang, *Validation of inter-particle collision models based on Large Eddy Simulation in gas-solid turbulent homogeneous shear flow*, in *Proc. 7<sup>th</sup> Int. Symp. Gas-Particle Flows, ASME Fluids Engng. Division Summer Meeting, Vancouver, 1997*, ASME paper FEDSM97-3623.
- [17] B.J. Legg, M.R. Raupach, *Markov-chain simulation of particle dispersion in inhomogeneous flows: the mean drift velocity induced by a gradient in Eulerian velocity variance*, *Boundary Layer Meteorol.*, 24 (1982), 3-13.
- [18] J.M. McInnes, F.V. Bracco, *Stochastic particle dispersion modeling and the tracer particle limit*, *Phys. Fluids A*, 4 (1992), 2809-2824.
- [19] L.P. Wang, D.E. Stock, *Dispersion of heavy particles by turbulent motion*, *J. Atmosph. Sci.*, 50 (1993), 1897-1913.
- [20] P. Rambaud, B. Oesterlé, A. Tanière, *Assessment of integral time scales in a gas-solid channel flow with relevance to particle dispersion modelling*, in M. Sommerfeld, ed., *Proc. 10<sup>th</sup> Workshop on Two-Phase Flow Predictions, Merseburg, Germany, 2002*, pp. 182-194.
- [21] Q. Wang, K.D. Squires, X. Wu, *Lagrangian statistics in turbulent channel flow*, *Atmos. Env.*, 29 (1995), 2417-2427.
- [22] T. Ushijima, R. Perkins, *Evaluation of  $C_0$  and  $T_L$  in turbulent pipe or channel flows*, in *Proc. ASME FED Summer Meeting, 3<sup>rd</sup> ASME/JSME Joint Fluids Engng. Conf., San Francisco, 1999*, ASME paper FEDSM99-7759.